

RESEARCH PAPER



Identifying a novel IRF3/circUHRF1/miR-1306-5p/ARL4C axis in pancreatic ductal adenocarcinoma progression

Wei Liu^{a,b,#}, Lisha Deng^{c,#}, Anchun Xu^{d,#}, Xingcheng Xiong^e, Jing Tao^e, Jian Chang^e, Yiling Xu^f, and Zhilin Zhou^g

^aDepartment of Medical Management, Sichuan Provincial People's Hospital, University of Electronic Science and Technology of China, Chengdu, China; ^bDepartment of Medical Management, Chinese Academy of Sciences Sichuan Translational Medicine Research Hospital, Chengdu, China; ^cDepartment of Neurosurgery, Hospital of Chengdu University of Traditional Chinese Medicine Chengdu, China; ^dDepartment of Clinical Laboratory, Hospital of Chengdu University of Traditional Chinese Medicine Chengdu, China; ^eDepartment of Pancreatic Surgery, Renmin Hospital of Wuhan University, Wuhan, China; ^fObstetrics and Gynecology Department, Liyuan Hospital, Tongji Medical College, Huazhong University of Science and Technology, Wuhan, China; ^gDepartment of General Surgery, Liyuan Hospital, Tongji Medical College, Huazhong University of Science and Technology, Wuhan, China

ABSTRACT

Pancreatic ductal adenocarcinoma (PDAC) is considered one most aggressive and lethal cancer types worldwide. While its underlying mechanisms are still poorly understood. CircRNAs play essential roles in various biological progression, including PDAC. Here, our results found that circUHRF1 was highly expressed in PDAC tumor tissues compared with normal tissues. Next, Cell or animal models were constructed, CCK-8, cell colony, EdU, flow cytometry assay, transwell migration, and Western blot assays were applied. CircUHRF1 knockdown influenced PDAC cell proliferation, apoptosis, migration and EMT level *in vitro*, and tumor growth *in vivo*. Subsequently, bioinformatics analysis, AGO2-RIP, RNA pull-down, and dual-luciferase reporter assays were used to explore the downstream targets in PDAC progression. Our findings suggest that circUHRF1 regulated ARL4C expression to promote PDAC progression through sponging miR-1306-5p. The role of miR-1306-5p in PDAC cellular progression has been elucidated, and the expression association between miR-1306-5p and circUHRF1 or ARL4C in PDAC tissues was analyzed. Furthermore, circUHRF1 expression in PDAC cells could be transcriptionally regulated by IRF3. Collectively, our study demonstrated the role of IRF3/circUHRF1/miR-1306-5p/ARL4C axis in PDAC progression. Our results suggest that circUHRF1 is one promising diagnosis or therapeutic target for PDAC management.

Abbreviations : CircRNA; Circular RNAPDAC; pancreatic ductal adenocarcinomaUHRF1; Ubiquitin-like with PHD and RING finger domain 1ARL4C; ADP Ribosylation Factor Like GTPase 4CRIP; RNA immunoprecipitationEDU; 5-Ethynyl-2'-deoxyuridineEMT; epithelial to mesenchymal transitionAGO2; Argonaute RISC Catalytic Component 2CCK8; Cell counting Kit-8IRF3; Interferon Regulatory Factor 3

ARTICLE HISTORY

Received 7 June 2021
Revised 29 August 2021
Accepted 9 December 2021

KEYWORDS





Circular RNA; circ UHRF1; miR-1306-5p; ARL4C; IRF3; pancreatic ductal adenocarcinoma

Introduction

Pancreatic ductal adenocarcinoma (PDAC) is one of the most aggressive and deadliest cancers, which causes fourth cancer-related death worldwide [1,2]. Due to the absence of early detection and insignificant early symptom, diagnosis of PDAC is often at an end-stage [3]. Despite the decades' efforts on the improvement of clinical management such as chemotherapy, immunotherapy, and gene target therapy. The survival rate of PDAC is still unfavorable, and the disease incidence is growing [4–7]. PDAC

has brought terrible life experiences to patients and a substantial economic burden for the world health care system. It is imperative to find novel targets for PDAC diagnosis and clinical intervention.

Circular RNAs (circRNAs) are a novel class of non-coding RNAs (ncRNA) family and are characterized by their covalently closed continuous loop structure, which is without 5'–3' polarity or poly(A) tail [8]. After decades of study, circRNAs were found abundantly, conservatively, and tissue specifically expressed in various species [9–11]. Mechanically,

CONTACT Yiling Xu  xuyiling2020@163.com  Obstetrics and Gynecology Department, Liyuan Hospital, Tongji Medical College, Huazhong University of Science and Technology, Wuhan, China; Zhilin Zhou  drzhouzhilin2021@163.com  Liyuan Hospital, Tongji Medical College, Huazhong University of Science and Technology, Wuhan, China

#: Co-first authors.

circRNAs exert their function mainly through interacting with microRNAs (miRNAs) or directly translating proteins [12,13]. Biologically, circRNAs play crucial roles in multiple cellular or disease progression, especially in cancer [14–16]. Recently, the role of circRNAs in PDAC progression has been widely studied. Guo X et al. demonstrated that circRNA circBFAR exerts its function in PDAC progression through miR-1306-5p/MET/Akt axis [17]. Wong CH et al. elucidated that circFOXK2 sponges to miR-942 and complexes with RNA-binding protein to aggravate growth and metastasis progression of PDAC [18]. Hao L et al. revealed that circ_0007534 regulates PDAC cellular progression via sponging miR-625 and miR-892b [19]. Accumulating evidence suggests that circRNAs exert an essential role in PDAC initiation or progression.

CircRNA Ubiquitin-like with PHD and RING finger domain 1 (circUHRF1) (hsa_circ_0048677) is spliced from the 12, 13 exons of UHRF1 gene and locates on chr19:4,950,622–4,951,008. Of interest, we notified that CircUHRF1 plays a crucial role in the progression of oral squamous cell carcinoma, hepatocellular carcinoma [20,21]. However, the role of circUHRF1 in PDAC progression remains uncovered. In the current study, we hypothesized that circUHRF1 exerts its function in PDAC progression. Firstly, circUHRF1 expression levels in PDAC tissues were measured. Next, by constructing circUHRF1 knock-down cell and mouse models, we investigated the biological role of circUHRF1 *in vitro* and *in vivo*. Subsequently, bioinformatics analysis, AGO2-RIP, RNA pull-down, and dual-luciferase reporter assays were performed to identify its down- and up-stream factors and underlying mechanisms. Collectively, our study partially demonstrated the promotive effect of circUHRF1 in PDAC progression.

Materials and methods

Clinical samples

A total of 26 PDAC tissues and 12 peritumoral normal tissues were collected from patients who underwent pancreaticoduodenectomy surgery at Renmin Hospital of Wuhan University between February 2018 and February 2019. Patients who received radiotherapy or chemotherapy or had other tumors were excluded. Tissue samples were stored at

–80°C after resection immediately. Adjacent normal tissues (2 cm always from tumor tissues) were collected and stored at –80°C as an internal control. Informed consent was obtained from all patients. All approaches were approved by the Ethics Committee of Renmin Hospital of Wuhan University.

Cell culture and transfection

PDAC cell lines (AsPC-1, PANC1, SW1990, BxPC3, and Hs766T), human pancreatic normal epithelial cell line HPDE and HEK-293 T were commercially obtained from Zeye Biotechnology (Shanghai, China). Cells were cultured by Roswell Park Memorial Institute (RPMI)-1640 medium, with 10% fetal bovine serum (FBS) (Gibco, USA) and 1% antibiotics at 37°C in a humidified atmosphere containing 5% CO₂. Lentivirus, siRNAs, and plasmids used in the study were synthesized and procured from GeneChem (Shanghai, China). The sequences of siRNAs are as following: Si-NC; TTCTCCGAACGTGTCACGT, Si-circUHRF1#1; GAGGATGATGTGGGATGAT, Si-circUHRF1#2; GATGTGGGATGATTCTCTG. Si-IRF3#1: F, 5'-CAGGAGGAUUUCGGA AUCUTT-3'; R, 5'-AGAUUCCGAAAUCCUCCU GTT-3'; Si-IRF3#2: F, 5'-GGAGGCAGUACUUCU GAUATT-3'; R, 5'-UAUCAGAAGUACUGCCUC CTT-3'; Si-NC: F, 5'-UUCUCCGAACGUGUCAC GUTT-3'; R, 5'-ACGUGACACGUUCGGAGAAT T-3'. All transfections were performed using Lipofectamine 3000 reagent (Invitrogen) according to the manufacturer's protocol.

RT-qPCR

TRIzol reagent (Invitrogen) was used to extract RNAs from samples and cells according to the manufacturer's protocol. Total RNAs were reverse transcribed into cDNA using the RevertAid First Strand cDNA Synthesis Kit (Thermo). RT-qPCR was carried out using the FastStart Universal SYBR Green Master (Rox) (Roche) in the ABI PRISM® 7300 real-time PCR system (Applied Biosystems, Foster City, CA, USA). The relative expression level was computed using 2- $\Delta\Delta C_t$ method. U6 and GAPDH were used as internal controls. Primers applied in the study are described as following: CircUHRF1; Forward primer (5'-3'), GCTATGAGGATGATGTGGGAT, and Reverse primer (5'-3'), CAGAGTCTGTTCACGTTCG

TCC. UHRF1: Forward primer (5'-3'), ATGACAC CATCCAGCTCCTGG, and Reverse primer (5'-3'), CTCATCCCACATGTCCTCATC. miR-1306-5p; Forward primer (5'-3'), GGCAGAGGAGGGCTGT TC, and Reverse primer (5'-3'), GTGCGTGTCGTGG AGTCG. ARL4C; Forward primer (5'-3'), CCAGTC CCTGCATATCGTCAT, and Reverse primer (5'-3'), TTCACGAACTCGTTGAACTTGA. GAPDH; Forward primer (5'-3'), GGAGCGAGATCCCTCCAAA AT, and Reverse primer (5'-3'), GGCTGTTGTCATA CTTCTCATGG. U6; Forward primer (5'-3'), CTCG CTTGGCAGCACA, and Reverse primer (5'-3'), AACGCTTACGAATTTGCGT.

RNase R treatment

RNase R was used to degrade linear RNA and amplified by a divergent primer. The treatment of RNase R was carried out according to the manufacturer's instructions. Briefly, total RNA (2 µg) after being extracted by Trizol reagent was incubated with 3 U/µg of RNase R for 15 min at 37°C, then treated RNA was purified with an RNA clean kit according to the instructions.

Western blot

Western blotting was carried out using standard techniques. Briefly, PDAC cells were washed twice with PBS and then lysed with ice-cold lysis buffer. The protein lysate was collected after centrifugation. The protein concentration was quantified using a Pierce™ BCA Protein Assay Kit according to the manufacturer's instruction. An equal quantity of protein lysate from each sample was analyzed by 10% SDS-PAGE, followed by protein transfer to PVDF membrane (Millipore). The membrane was then incubated with primary antibodies overnight at 4°C, washed, and incubated with secondary antibodies. Protein expression was detected using the using UVP imaging system (UVP, LLC, Upland, CA, USA). Antibodies used in study are listed as following: E-cadherin (CST; 14472S; 1:1000), Vimentin (CST; 5741S; 1:1000), ARL4C (Abcam; ab122025; 1:500), GAPDH (CST; 5174S; 1:1000).

CCK-8 assay

The cell proliferation was assessed by Cell counting Kit-8 (CCK-8) (Beyotime, Shanghai, China) according to the manufacturer's instruction. Transfected cells were seeded in 96-well plates and cultured at 37°C with 5% CO₂ overnight. After 0, 24, 48, 72 hours incubation, the CCK-8 reagent was added into each and cultured for 2 hours. The absorbance was measured at 450 nm by using a Microplate reader.

Cell colony formation assay

For cell colony formation assay, transfected cells were cultured in 6-well plates at 37°C with 5% CO₂ overnight. After 2 weeks, we washed cells two times with PBS and fixed cells with 4% paraformaldehyde for 20 min and then stained the cells with 0.1% crystal violet for 15 min. Then colony numbers were manually counted.

5-Ethynyl-2'-deoxyuridine (EdU)

The EdU assay was carried out to assess the proliferation viability of cells using a BeyoClick™ EdU-555 detection kit (Beyotime, Shanghai, China). Transfected cells were cultured in 12-well plates and incubated with medium for 12 h. After incubation with EdU for 2 h, the cells were fixed and stained for 30 minutes. Blue-fluorescent nuclear counterstain-Hoechst 33,342 was used to stain the nucleic acid. Images were captured with a fluorescent microscope.

Flow cytometry assay

The apoptotic rate of transfected PANC1 and AsPC-1 cells was detected by conducting a Flow cytometry assay using an Annexin V-fluorescein isothiocyanate (FITC)/propidium iodide (PI) apoptosis detection kit (Solarbio, China) following the instructions from the manufacture. In summary, after transfection, cells were subjected to FITC-labeled annexin V and PI for incubation and followed by the fluorescence intensity measurement under a flow cytometry (BD Biosciences, USA). The experiment was performed in triplicate.

TRANSWELL assay

The cell migration was assessed by transwell assay following the manufacturer's instruction. Cells were seeded into the upper chamber in FBS-free media with membrane inserts without Matrigel. 0.6 ml DMEM supplemented with 10% FBS as the attractant was added into the lower chamber. After incubation 24 hours at 37°C, top chamber cells were removed, cells in the lower chamber were fixed with 4% paraformaldehyde and stained with crystal violet for 20 min. The number of cells was counted under a microscope (Olympus, Tokyo, Japan). Experiments were performed at least three times.

Animal experiment

A total of 54 BALB/c-nu/nu mice (5–6 weeks, 20–22 g) were commercially obtained from Beijing Vital River Laboratory Animal Technology (Beijing, China). All mice were randomly separated into three groups (n = 6). Mice were subcutaneously injected with PANC1 cells (10⁶ per mouse) pre-transfected with Si-NC, Si-circUHRF1#1, and Si-circUHRF1#2. The volumes of all tumor xenografts were recorded 4 days a time. Mice were sacrificed four weeks after injection. Tumor end weights were measured. Pancreas tissues were fixed in 4% paraformaldehyde, embedded in paraffin, and sectioned.

RNA immunoprecipitation (RIP)

RNA immunoprecipitation was performed by Magna RIP™ RNA-Binding Protein Immunoprecipitation Kit (Millipore) according to the manufacturer's protocol. Cells were harvested in RIP lysis buffer, and the lysates were stored at – 80°C. Magnetic beads were washed twice with RIP wash buffer, followed by incubation with 2 µg antibody for 30 mins at room temperature. Immunoprecipitation was performed by incubating cell lysate with the magnetic bead-antibody complex overnight at 4 °C. The beads were further mixed with proteinase K buffer and incubated for 30 min at 55°C, and RNA was finally purified for PCR use.

Biotinylated RNA pull-down

RNA Pull-down assay was performed using Pierce Magnetic RNA-Protein Pull-Down Kit (ThermoFisher Scientific). Cells were harvested and fixed with 1% formaldehyde, and then washed by PBS, and lysed in lysis buffer. The biotinylated probe was incubated with streptavidin-coated magnetic beads (Invitrogen, Waltham, MA, USA) for 2 h and added to cell lysates for incubation overnight at 4°C. Then, the mixture was washed with lysis buffer and added into RNAiso Plus (Takara, Japan) to extract RNAs. RNAs were reverse transcript by RT reagent Kit (RR047A, Takara, Japan). RT-qPCR assays were performed by using the TB Green Premix Ex Taq™ kit (Takara).

Luciferase reporter assay

Cells pre-transfected with luciferase reporter vectors harboring wildtype (WT) or mutated type (MUT) sequences were seeded in 96-well plate and. Cells were washed with iced PBS two times. The luciferase activity was measured by the Dual-Luciferase Reporter Assay System (Promega, USA), following the manufacturer's instructions.

Statistical analysis

The statistical analysis was implemented by SPSS 22.0 statistical software (IBM, Armonk, NY, USA). The data were presented as Mean ± SD. Student's t-test or one-way analyses of variance (ANOVA) was used to compare group differences. Spearman analysis was used to calculate the association between miR-1306-5p and circUHRF1 or ARL4C expression in PDAC tumor tissues. $p < 0.05$ was considered as a statistical difference.

Results

Expression of circUHRF1 in PDAC

Bioinformatics analysis showed that circUHRF1 is an exonic circRNA that is cyclized with the 12, 13 exons of the UHRF1 gene (Figure 1(a)). The expression level of circUHRF1 in 12 normal tissues

and 26 PDAC tissues was measured. CircUHRF1 was highly expressed in PDAC tumor tissues compared with normal tissues (Figure 1(b)). Next, circUHRF1 was found abundantly expressed in PDAC cell lines (Hs766T, PANC1, SW1990, BxPC3, and AsPC-1) compared with pancreatic epithelial cell line HPDE. Subsequently, the circular RNA characteristics of circUHRF1 were experimentally verified. Firstly, reverse transcription experiments were conducted using random hexamer or oligo (dT)18 primers. Upon the treatment of oligo (dT)18 primers, circUHRF1 expression level was obviously lower than random hexamer primers treatment, suggested that circUHRF1 structurally has no poly-A-tail (Figure 1(d)). Next, circUHRF1 obviously resisted RNase R digestion in comparison with UHRF1 (Figure 1(e)). The transcription inhibitor actinomycin D was applied to assess the half-time of circUHRF1 and UHRF1 in PANC1 cells; it was found that circUHRF1 was more stable than UHRF1 (Figure 1(f)). The location of circUHRF1 in PANC1 cells was detected using cellular RNA fractionation. The results showed that circUHRF1 was mainly distributed in the cytoplasm of PANC1 cells (Figure 1(g)).

Downregulation of circUHRF1 suppresses PDAC cellular progression and reverses the EMT process

To explore whether circUHRF1 exerts its role in PDAC progression. CircUHRF1 knockdown cell models were constructed, and transfection efficiencies were assessed (Figure 2(a)). We utilized CCK-8 (Figure 2(b,c)), EdU (Figure 2(d)), Cell colony formation (Figure 2(e)), and Flow cytometry assays (Figure 2(f)). We found that circUHRF1 knockdown significantly suppressed cell proliferation ability and promoted cell apoptosis rate. The results of the Transwell migration assay indicated that circUHRF1 knockdown inhibited cell migration level (Figure 2(g)). Further, the epithelial to mesenchymal transition (EMT) level in cell models were assessed. E-cadherin was upregulated in circUHRF1 knockdown cells, while Vimentin was downregulated (Figure 2(h)). Here, our results indicate that the inhibitory effects of circUHRF1 knockdown on PDAC cellular progression. Subsequently, the role of circUHRF1 *in vivo* was evaluated by constructing circUHRF1 knockdown animal models. As the representative

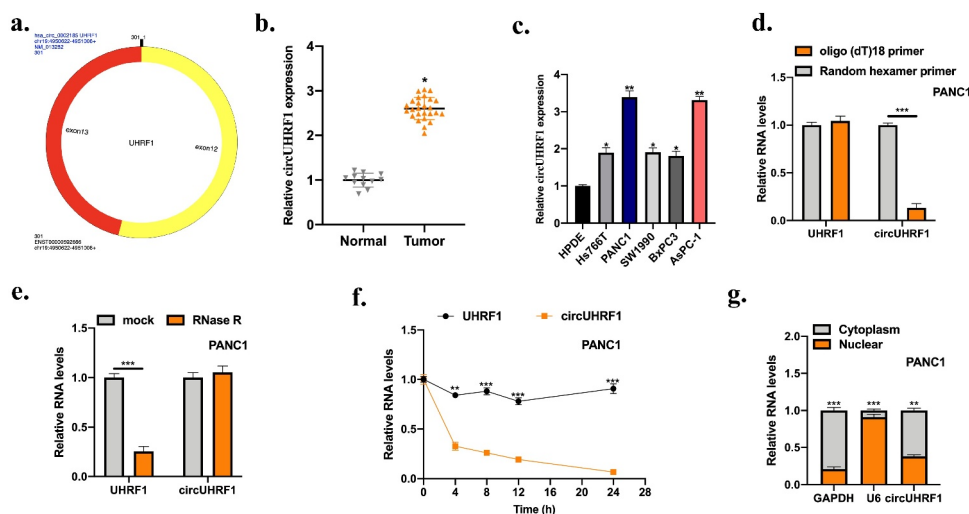


Figure 1. Expression of circUHRF1 in PDAC. a: The diagram information of circUHRF1 was shown. b: Measurement of circUHRF1 expression in adjacent normal tissues ($n = 12$) and PDAC tissues ($n = 26$) was examined by qRT-PCR. c: Measurement of circUHRF1 expression in PDAC cell lines (AsPC-1, PANC1, SW1990, BxPC3, and Hs766T) in comparison with pancreatic epithelial cell line HPDE was detected using qRT-PCR. d: Random hexamer or oligo (dT)18 primers were used for reverse transcription assays. RT-qPCR was used to examine the relative RNA levels. e: After treatment with actinomycin d at the indicated time points in PANC1 cells, RT-PCR was conducted to measure the relative RNA levels. f: After treatment with RNase R or mock in total RNAs derived from PANC1 cells. Relative RNA levels were examined by RT-qPCR. g: Relative expression of circUHRF1 in nuclear and cytoplasm. All experiments were performed three times, and data were presented as mean \pm SD. * $p < 0.05$, ** $p < 0.05$, *** $p < 0.001$.

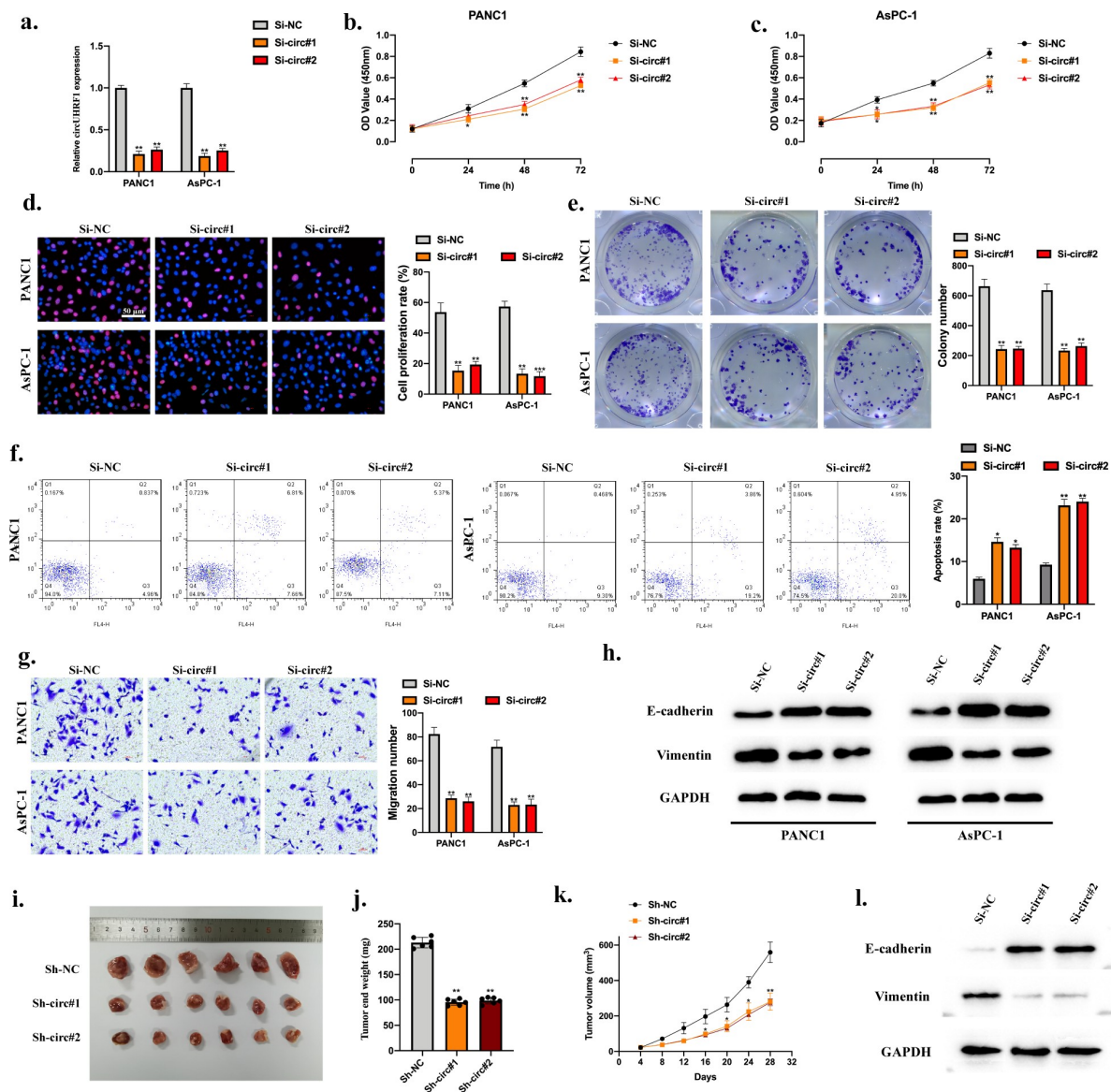


Figure 2. Downregulation of circUHRF1 suppresses PDAC cellular progression and reverses the EMT process. a: We stably transfected Sh-NC, Sh-circ#1, and Sh-circ#2 into PANC1 and AsPC-1 cells; results were evaluated by qRT-PCR. b-e: Cell proliferation abilities of transfected cells were detected by CCK-8 (b-c), EdU (d), and Colony formation assays (e). f: Cell apoptotic rates were evaluated by Flow cytometry assay; results were statistically analyzed. g: Cell migration abilities were detected by TRANSWELL assay. h: The EMT-related proteins in indicated groups were measured by Western blot. Nude mice were randomly separated into three groups (n = 6) and subcutaneously injected with PANC1 (10^6 per mouse) cells pre-transfected with Si-NC, Si-circUHRF1#1, Si-circUHRF1#2. i: Representative image of subcutaneously incubated tumors (n = 6). j: Tumor volumes were recorded three days a time and presented. k: Tumor end weights were recorded, and comparative statistics were shown. l: The EMT-related proteins in tumor tissues were detected by Western blot assay. All experiments were performed three times, and data were presented as mean \pm SD. * $p < 0.05$, ** $p < 0.01$.

images of the subcutaneous tumors showed that circUHRF1 knockdown significantly inhibited tumor growth *in vivo* (Figure 2(i)). Tumor end weights, volumes and, the EMT phenomena were inhibited by circUHRF1 knockdown (Figure 2(j,k)).

CircUHRF1 functions as a sponge of miR-1306-5p

The above results demonstrated that circUHRF1 plays its role in PDAC progression both *in vitro* and *in vivo*. While its underlying mechanisms remain unclear. AGO-2 RIP assay was conducted, and we found that

circUHRF1 was significantly enriched in AGO-2 antibody compared with IgG antibody, suggested that circUHRF1 might bind with miRNA (Figure 3(a)). Bioinformatics analyses were applied to find putative downstream targets for circUHRF1, predicted miRNAs were selected for biotinylated RNA pull-down assay. MiR-1306-5p was obviously enriched in the bio-circUHRF1 probe compared with bio-NC probes, indicated that miR-1306-5p might be a downstream target for circUHRF1 (Figure 3(b)).

Subsequently, the binding sites between circUHRF1 and miR-1306-5p were synthesized (Figure 3(c)). Dual-luciferase reporter assays showed that miR-1306-5p mimic significantly inhibited luciferase activities in HEK-293 T and PANC1 cells pre-transfected circUHRF1 MUT reporter vectors (Figure 3(d)), suggested that circUHRF1 sponges miR-1306-5p. Moreover, the miR-1306-5p expression level in PANC1 and AsPC-1 cells was negatively regulated by circUHRF1 (Figure 3(e)). MiR-1306-5p

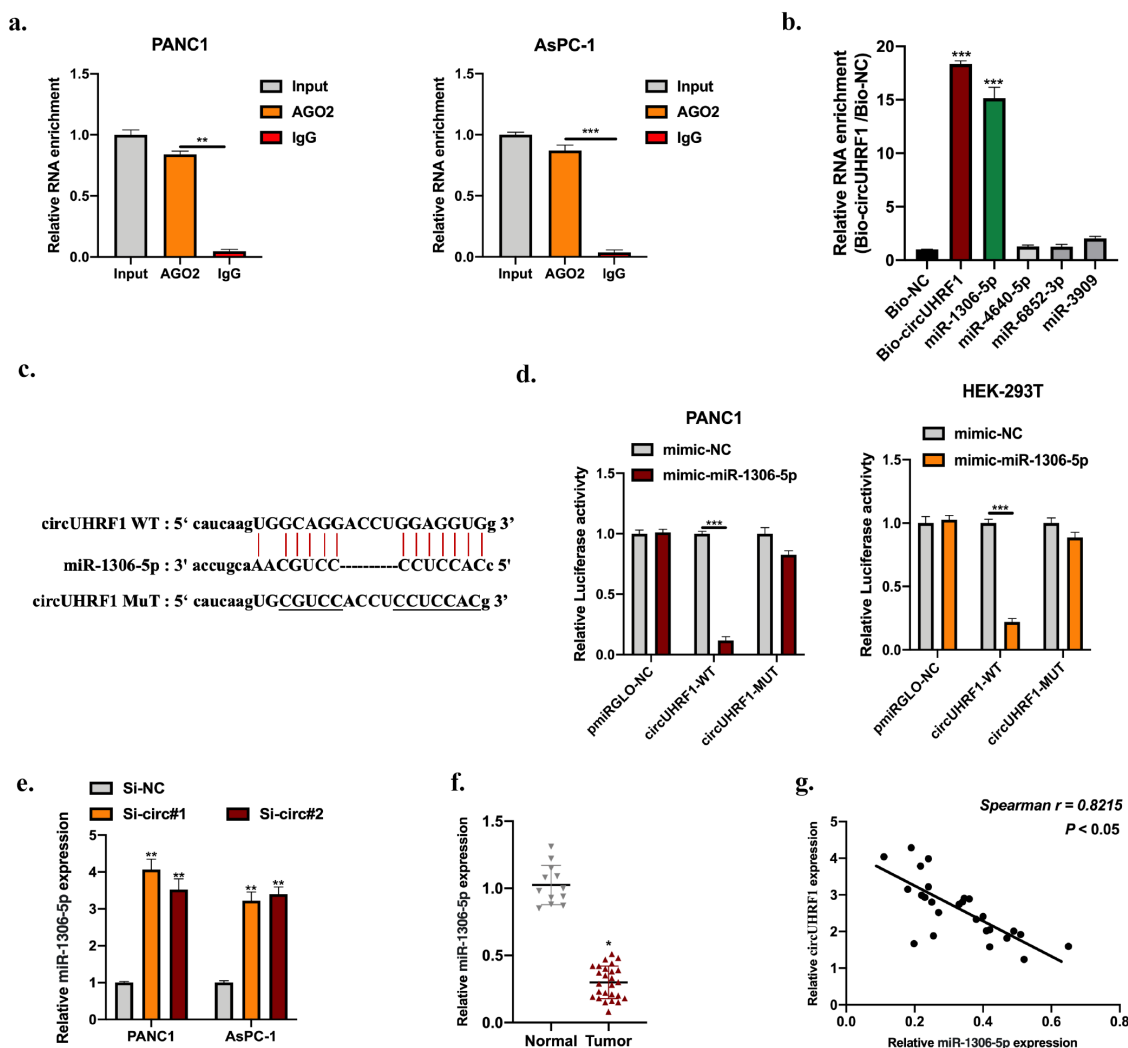


Figure 3. CircUHRF1 functions as a ceRNA of miR-1306-5p. ENCORI database was used to predict putative downstream miRNA targets for circUHRF1. (<http://starbase.sysu.edu.cn>, CLIP data: high stringency (≥ 3)). a: RNA immunoprecipitation (RIP) and RT-qPCR assays were conducted to analyze the binding capability of circUHRF1 to AGO2 protein in PANC1 (a) and AsPC-1 (b) cells. B: RNA pull-down assay using Bio-NC probes and Bio-circUHRF1 probes was performed to detect putative miRNA levels in PANC1 cells. c: The predicted binding sites between circUHRF1 and miR-1306-5p were shown. d: Relative luciferase activity measurement in HEK-293 T cells and PANC1 cells transfected with miR-1306-5p mimic and reporter vectors harboring WT or Mut circUHRF1 sequences. e: Relative expression of miR-1306-5p in circUHRF1 knockdown PANC1 and AsPC-1 cells was measured by qRT-PCR. f: Relative expression of miR-1306-5p in adjacent normal tissues ($n = 12$) and PDAC tissues ($n = 26$) was detected by qRT-PCR. g: The expression correlation between circUHRF1 and miR-1306-5p in PDAC tissues was statistically calculated using spearman analysis. All experiments were performed three times, and data were presented as mean \pm SD. * $p < 0.05$, ** $p < 0.01$, *** $p < 0.001$.

expression in PDAC tumor tissues was obviously lower than normal tissues and statistically associated with circUHRF1 expression (Figure 3(f,g)).

MiR-1306-5p inhibits PDAC cellular progression and reverses the EMT process

Here, we investigated the role of miR-1306-5p in PDAC development. MiR-1306-5p overexpression cell models were generated, the miR-1306-5p

expression level in cell models was detected (Figure 4(a)). MiR-1306-5p overexpression obviously inhibited PDAC cell proliferation level using CCK-8 (Figure 4(b)), cell colony (Figure 4(c)), and EDU (Figure 4(d)) assays. Results of the Flow cytometry assay shown that miR-1306-5p overexpression markedly promoted the PDAC cell apoptotic rate (Figure 4(e)). The migration ability of PDAC cells was suppressed upon miR-1306-5p overexpression (Figure 4(f)).

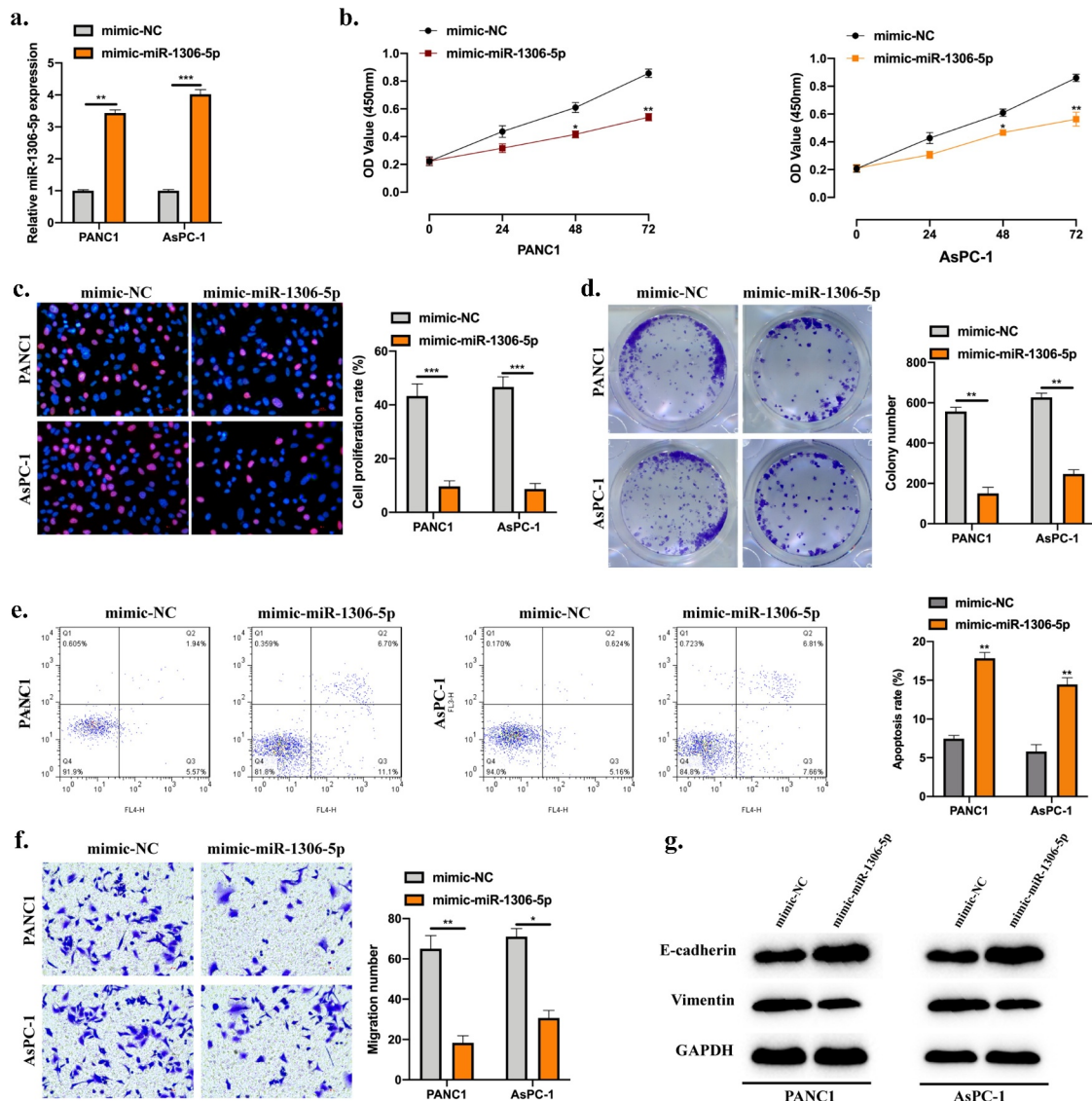


Figure 4. MiR-1306-5p inhibits PDAC cellular progression and reverses the EMT process. a: MiR-1306-5p overexpression cell models were constructed by stably transfecting miR-1306-5p mimics and its normal control mimics into PANC1 and AsPC-1 cells. Transfection results were detected by qRT-PCR. B-D: CCK-8 (b), EdU (c), and Colony formation assays (d) were performed to evaluate cell proliferation abilities. e: Apoptotic rates of transfected cells were evaluated by Flow cytometry assay. f: Transwell assay was applied to measure cell migration levels. F: Western blot was conducted to detect the EMT-related proteins in indicated groups. All experiments were performed three times, and data were presented as mean \pm SD. * $p < 0.05$, ** $p < 0.01$, *** $p < 0.001$.

Moreover, the inhibitive phenomenon of miR-1306-5p overexpression coupled with upregulated E-cadherin and downregulated Vimentin in PDAC cell lines (Figure 4(g)).

MiR-1306-5p directly targets ARL4C

According to bioinformatics analysis results, the putative mRNA targets of miR-1306-5p were selected. Biotinylated RNA pull-down using bio-miR-1306-5p probes and bio-NC probes were conducted. ADP Ribosylation Factor Like

GTPase 4 C (ARL4C) was significantly enriched in bio-miR-1306-5p probes (Figure 5(a)). The WT or MUT binding sites between miR-1306-5p and ARL4C were synthesized (Figure 5(b)). Dual-luciferase reporter assays showed that miR-1306-5p mimic obviously suppressed luciferase activities in HEK-293 T and PANC1 cells pre-transfected ARL4C MUT reporter vectors (Figure 5(c,d)). The expression of ARL4C in PDAC cells was negatively regulated by miR-1306-5p (Figure 5(e,f)). Moreover, ARL4C expression level was upregulated in PDAC

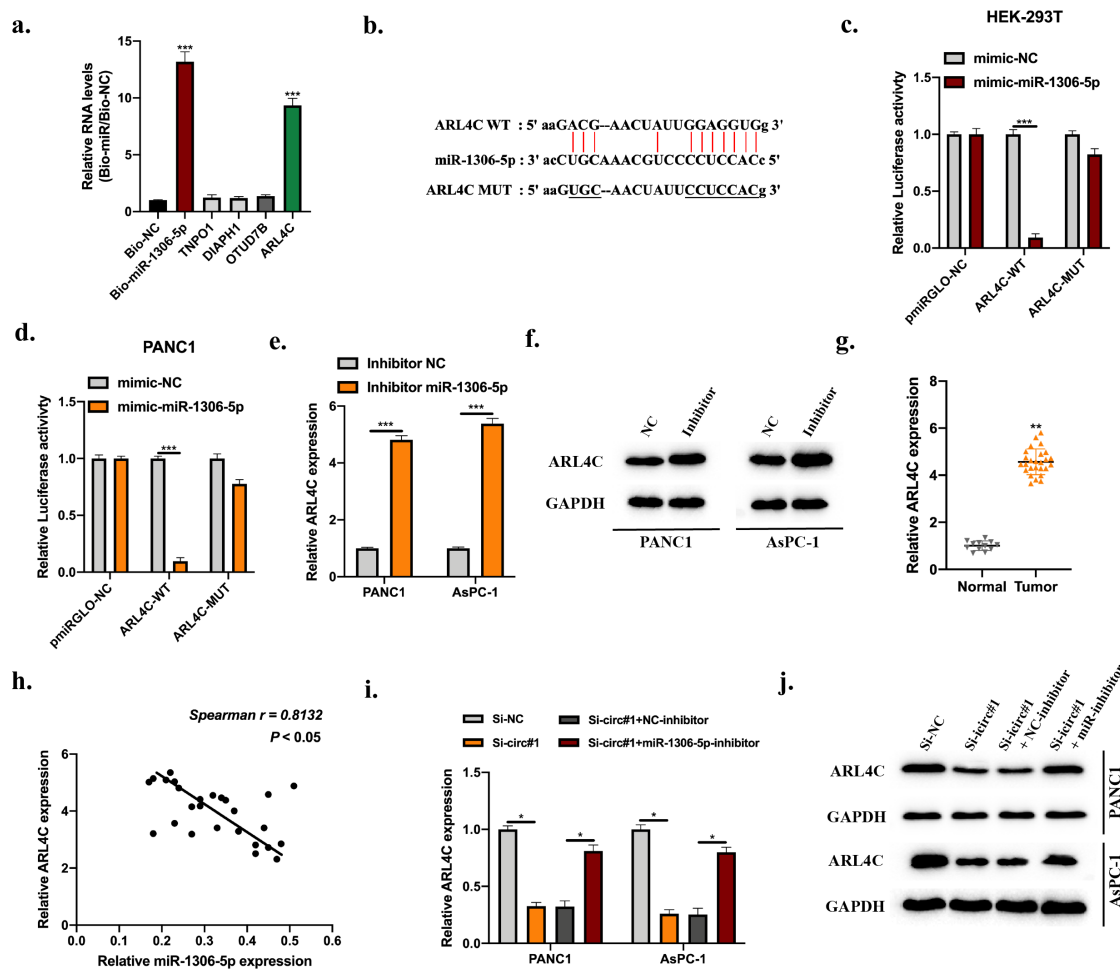


Figure 5. MiR-1306-5p directly targets ARL4C. Bioinformatics analysis were conducted using miRanda (<http://www.mirbase.org>), miRmap (<https://mirmap.ezlab.org>), and TargetScan (http://www.targetscan.org/mamm_31) with CLIP data: strict stringency (≥ 5), Degradome data: low stringency (≥ 1). Putative targets were selected. A: RNA pull-down using Bio-NC probes and Bio-miR-1306-5p probes to detect putative mRNAs' level. b: The predicted binding sites between miR-1306-5p and ARL4C were shown. c-d: Relative luciferase activities in HEK-293 T and PANC1 cells transfected with miR-1306-5p mimic and reporter vectors harboring WT or Mut ARL4C sequences were measured. e-f: ARL4C levels in PANC1 and AsPC-1 cells stably transfected with miR-1306-5p inhibitors, and their normal control was measured by qRT-PCR and Western blot assays. g: ARL4C levels in adjacent normal tissues ($n = 12$) and PDAC tissues ($n = 26$) were measured by qRT-PCR. H: The expression correlation between miR-1306-5p and ARL4C in PDAC tissues was calculated by spearman analysis. i-j: ARL4C expression in Si-NC, Si-circ#1, Si-circ#1 + NC-inhibitor, Si-circ#1 + miR-1306-5p-inhibitor transfected PANC1, and AsPC-1 cells were measured by RT-qPCR and Western blot. All experiments were performed three times, and data were presented as mean \pm SD. * $p < 0.05$, ** $p < 0.01$, *** $p < 0.001$.

tumor tissues compared with normal tissues (Figure 5(g)) and statistically correlated with miR-1306-5p expression (Figure 5(h)). ARL4C expression in PDAC cells was inhibited by circUHRF1 knockdown but reversed by miR-1306-5p knockdown (Figure 5(i,j)).

CircUHRF1 knockdown decreases ARL4C expression to inhibit PDAC progression via sponging miR-1306-5p

To assess the role of circUHRF1/miR-1306-5p/ARL4C pathway in PDAC progression. We constructed cell models as indicated, transfection efficiencies were assessed (Figure 6(a)). By

conducting CCK-8 (Figure 6(b,c)), EDU (Figure 6(d,e)), and cell colony (Figure 6(f,g)) assays, we found that the inhibitory effect of circUHRF1 knockdown on PDAC cell proliferation was rescued by ARL4C overexpression. Results of the Flow cytometry assay also shown upregulated ARL4C attenuated the promotive effect of circUHRF1 knockdown on PDAC cell apoptosis (Figure 6(h,i)). For the same phenomena, circUHRF1 knockdown suppressed PDAC cell migration while reversed by ARL4C overexpression (Figure 6(j,k)). Further, the effects of circUHRF1 knockdown on E-cadherin and Vimentin expression were rescued by ARL4C overexpression (Figure 6(l)).

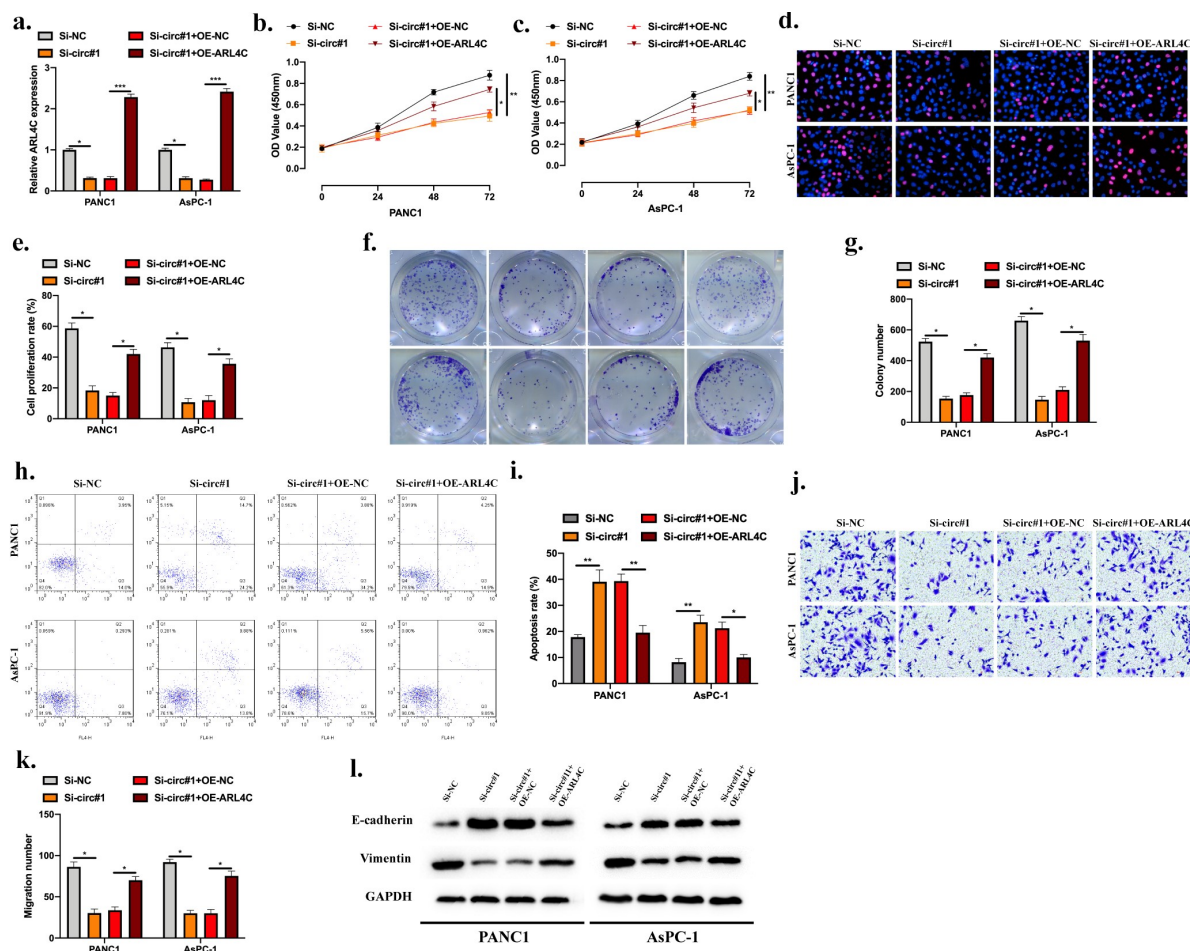


Figure 6. CircUHRF1 knockdown decreases ARL4C expression to inhibit PDAC progression via sponging miR-1306-5p. a: PANC1 and CFPAC1 cells were stably transfected with Si-NC, Si-circ#1, Si-circ#1 + OE-NC, Si-circ#1 + OE-ARL4C as indicated, transfection efficiencies were detected by RT-qPCR. B-G: CCK-8 (b-c), EdU (d-e), and Colony formation assays (f-g) were performed to evaluate cell proliferation abilities. h-i: Cell apoptotic rate was evaluated by Flow cytometry assay. j-k: Transwell assay was applied to measure cell migration levels. l: Western blot was conducted to detect the EMT-related protein levels in indicated groups. All experiments were performed three times, and data were presented as mean \pm SD. * $p < 0.05$, ** $p < 0.01$, *** $p < 0.001$.

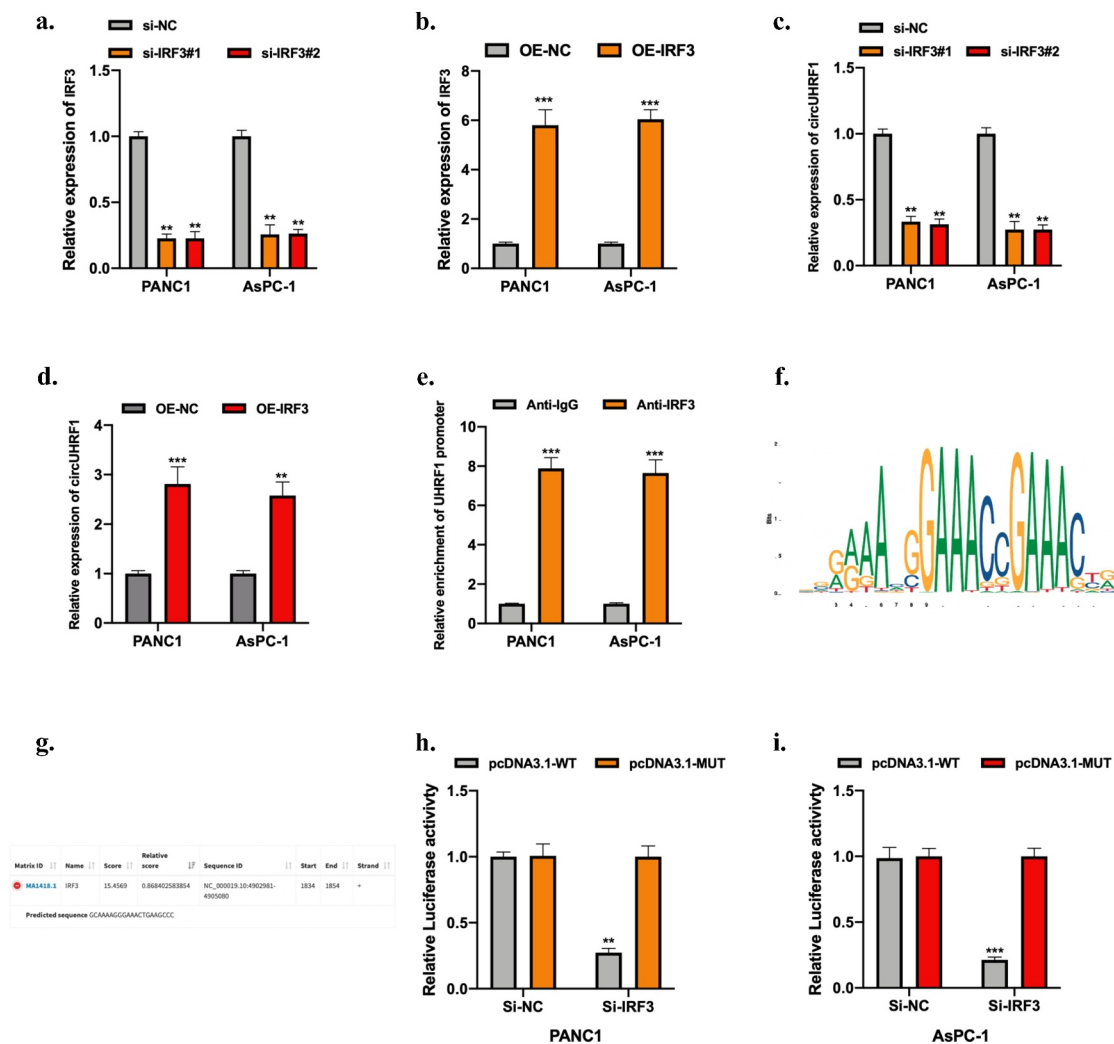


Figure 7. IRF3 mediates circUHRF1 expression in PDAC cells. a-b: PANC1 and AsPC-1 cells were stably transfected siRNAs (si-IRF3#1 and si-IRF3#2) targeting IRF3, and lentivirus containing IRF3 vector (OE-IRF3), and their normal controls. Transfection results were tested using the qRT-PCR assay. c-d: CircUHRF1 expression in IRF3 knockdown or overexpressed PDAC cells was measured by qRT-PCR assay. e: RIP assay using anti-IgG and anti-IRF3 antibodies was conducted, results were analyzed using the qRT-PCR assay. f: The putative binding domain of IRF3 was obtained from the JASPAR database. g: The predicted binding region of the UHRF1 promoter on IRF3 was obtained from the JASPAR database. h-i: The relationship between IRF3 and UHRF1 promoter was assessed by luciferase reporter gene assay. All experiments were performed three times, and data were presented as mean \pm SD. ** p < 0.01, *** p < 0.001.

CircUHRF1 regulated ARL4C expression to promote PDAC progression through sponging miR-1306-5p.

IRF3 mediates circUHRF1 expression in PDAC cells

Our results have elucidated the functional role of circUHRF1 in PDAC progression and the downstream molecular mechanisms. Here, we further investigated the upstream regulator of circUHRF1 in PDAC. Bioinformatics analysis using the JASPAR (<http://jaspar.genereg.net>) database

showed that Interferon Regulatory Factor 3 (IRF3) is a promising transcription factor of circUHRF1. Next, we explored the relationship between them. Firstly, we generated IRF3 knockdown and overexpression PDAC cell models as shown in Figure 7(a,b). Results of the qRT-PCR experiment shown that circUHRF1 expression could be positively regulated by IRF3 in PDAC cells (Figure 7(c,d)). Next, Results of the RIP assay indicated that UHRF1 promoter markedly enriched in anti-IRF3 bounds compared with anti-IgG in PANC1 and AsPC-1 cells (Figure 7(e)). We obtained the putative binding domain of IRF3

(Figure 7(f)) and UHRF1 promoter (Figure 7(g)) from the JASPAR database. Luciferase reporter gene assay was conducted, and the interaction between IRF3 and UHRF1 promoter was confirmed in PDAC cells (Figure 7(h,i)).

Discussion

With the development of high-throughput sequencing technology in recent years, numerous of circRNAs have been identified and investigated [22,23]. While there only are few circRNAs have been studied in PDAC. In this study, we hypothesized that circUHRF1 exerts its role in the progression of PDAC. CircUHRF1 was highly expressed in PDAC tumor tissues and cells. The circular RNA characterizations of circUHRF1 were identified using Random hexamer or oligo (dT)18 primers, actinomycin D treatment, and RNase R treatment. Our results suggest that circUHRF1 might play its functional role in PDAC progression. Furthermore, our results showed that circUHRF1 knockdown influenced PDAC cell proliferation, apoptosis, migration, EMT level *in vitro*, and tumor growth *in vivo*.

Next, we explored the downstream targets of circUHRF1 in PDAC cells. Among the investigation of molecular mechanisms of circRNAs in various cellular progressions, the circRNA/miRNA/mRNA network shows its indispensable contribution. The molecular mechanisms of circRNA/miRNA/mRNA network have been well documented in multiple tumorigenesis, for instance, in Lung cancer, Hepatocellular carcinoma, Oral squamous carcinoma, Gastric cancer [24–27]. In PDAC, the circRNA/miRNA/mRNA network has also been elucidated [28–30]. Hence, we focused on the ceRNA molecular role of circUHRF1 in PDAC. AGO2-RIP, bioinformatic analysis, RNA pull-down, and dual-luciferase reporter assays were conducted. We found that circUHRF1 sponged miR-1306-5p and negatively regulated its expression in PDAC cell lines.

MiR-1306-5p functional roles in multiple diseases have been investigated [31–35]. To our knowledge, the role of miR-1306-5p in tumorigenesis progression of PDAC remains uncovered. Here, we identified miR-1306-5p as a downstream target of circUHRF1. MiR-1306-5p

overexpression influenced PDAC cell proliferation, apoptosis, migration, and EMT level. The miR-1306-5p expression level was decreased in PDAC tumor tissues compared with normal tissues and statistically correlated with circUHRF1 expression. Bioinformatics analysis, biotinylated RNA pull-down, and dual-luciferase reporter assays were used to identify the mRNA target of miR-1306-5p in PDAC cells. MiR-1306-5p targeted ARL4C and negatively regulated its expression in PDAC cells. ARL4C was highly expressed in PDAC tumor tissues and associated with miR-1306-5p expression. Overexpression of ARL4C reversed the biological effect of circUHRF1 knockdown on cell proliferation, apoptosis, migration, and EMT level.

Our results have demonstrated the downstream mechanisms of circUHRF1 in PDAC. The upstream regulator was also investigated further to understand the biological pattern of circUHRF1 in PDAC. Previous studies have elucidated that transcription factor plays an important role in circRNA expression. The biogenesis of circSEPT9 in Triple-negative breast cancer could be mediated by E2F1 and EIF4A3 [36]. The stability and expression of circular ARF1 in glioma stem cells were bound and promoted by U2AF2 [37]. CircRNA_001160 expression in glioma endothelial cells could be promoted by PTBP1 [38]. Hence, to discover whether circUHRF1 expression in PDAC cells is regulated by a transcription factor, we utilized the JASPAR database. Of interest, we found that IRF3 might bind to the promoter region of UHRF1. Serial experiment results showed that circUHRF1 expression in PDAC cells could be positively regulated by IRF3, and IRF3 directly binding to the promoter domain of UHRF1 in PDAC cells.

Although the demonstration of the role of IRF3/circUHRF1/miR-1306-5p/ARL4C axis in PDAC progression has been partially revealed, an in-depth investigation was demanded in our study. Clinical analysis needs to be further confirmed by a larger sample number. The specific clinical information of enroll patients need carefully following up. The underlying mechanisms of ARL4C in PDAC progression are waiting for investigation in our future study.

Collectively, our study results partially demonstrated the role of circUHRF1 in PDAC progression. CircUHRF1 induced by IRF3 regulated ARL4C expression to promote PDAC progression through sponging miR-1306-5p. We might provide promising targets for PDAC diagnosis and therapy.

Disclosure statement

No potential conflict of interest was reported by the author(s).

Data availability statement

The data that support the findings of this study are available from the corresponding author upon reasonable request.

Funding

This work was supported by the Supported by Hospital of Chengdu University of Traditional Chinese Medicine Scientific Development Fund Project (20ZYTS06).

References

- [1] Siegel RL, Miller KD, Jemal A. Cancer Statistics, 2017. *CA Cancer J Clin.* 2017;67(1):7–30.
- [2] Hidalgo M. Pancreatic cancer. *N Engl J Med.* 2010;362(17):1605–1617.
- [3] Siegel RL, Miller KD, Jemal A. Cancer statistics, 2018. *CA Cancer J Clin.* 2018;68(1):7–30.
- [4] Ryan DP, Hong TS, Bardeesy N. Pancreatic adenocarcinoma. *N Engl J Med.* 2014;371(11):1039–1049.
- [5] Gupta R, Amanam I, Chung V. Current and future therapies for advanced pancreatic cancer. *J Surg Oncol.* 2017;116(1):25–34.
- [6] Dutta P, Perez MR, Lee J, et al. Combining hyperpolarized real-time metabolic imaging and NMR spectroscopy to identify metabolic biomarkers in pancreatic cancer. *J Proteome Res.* 2019;18(7):2826–2834.
- [7] Momeny M, Esmaili F, Hamzehlou S, et al. The ERBB receptor inhibitor dacomitinib suppresses proliferation and invasion of pancreatic ductal adenocarcinoma cells. *Cell Oncol (Dordr).* 2019;42(4):491–504.
- [8] Jeck WR, Sorrentino JA, Wang K, et al. Circular RNAs are abundant, conserved, and associated with ALU repeats. *RNA.* 2013;19(2):141–157.
- [9] Zhou R, Wu Y, Wang W, et al. Circular RNAs (circRNAs) in cancer. *Cancer Lett.* 2018;425:134–142.
- [10] Matsumoto Y, Fishel R, Wickner RB. Circular single-stranded RNA replicon in *Saccharomyces cerevisiae*. *Proc Natl Acad Sci U S A.* 1990;87(19):7628–7632.
- [11] Danan M, Schwartz S, Edelheit S, et al. Transcriptome-wide discovery of circular RNAs in Archaea. *Nucleic Acids Res.* 2012;40(7):3131–3142.
- [12] Thomas LF, Saetrom P. Circular RNAs are depleted of polymorphisms at microRNA binding sites. *Bioinformatics.* 2014;30(16):2243–2246.
- [13] Kallen AN, Zhou XB, Xu J, et al. The imprinted H19 lncRNA antagonizes let-7 microRNAs. *Mol Cell.* 2013;52(1):101–112.
- [14] Rajappa A, Banerjee S, Sharma V, et al. Circular RNAs: emerging role in cancer diagnostics and therapeutics. *Front Mol Biosci.* 2020;7:577938.
- [15] Tabatabaieian H, Peiling Yang S, Tay Y. Non-coding RNAs: uncharted mediators of thyroid cancer pathogenesis. *Cancers (Basel).* 2020;12(11):3264.
- [16] Goodall GJ, Wickramasinghe VO. RNA in cancer. *Nat Rev Cancer.* 2020;21(1):22–36.
- [17] Guo X, Zhou Q, Su D, et al. Circular RNA circBFAR promotes the progression of pancreatic ductal adenocarcinoma via the miR-34b-5p/MET/Akt axis. *Mol Cancer.* 2020;19(1):83.
- [18] Wong CH, Lou UK, Li Y, et al. CircFOXK2 promotes growth and metastasis of pancreatic ductal adenocarcinoma by complexing with RNA-binding proteins and sponging MiR-942. *Cancer Res.* 2020;80(11):2138–2149.
- [19] Hao L, Rong W, Bai L, et al. Upregulated circular RNA circ_0007534 indicates an unfavorable prognosis in pancreatic ductal adenocarcinoma and regulates cell proliferation, apoptosis, and invasion by sponging miR-625 and miR-892b. *J Cell Biochem.* 2019;120(3):3780–3789.
- [20] Zhang PF, Gao C, Huang XY, et al. Cancer cell-derived exosomal circUHRF1 induces natural killer cell exhaustion and may cause resistance to anti-PD1 therapy in hepatocellular carcinoma. *Mol Cancer.* 2020;19(1):110.
- [21] Zhao W, Cui Y, Liu L, et al. Splicing factor derived circular RNA circUHRF1 accelerates oral squamous cell carcinoma tumorigenesis via feedback loop. *Cell Death Differ.* 2020;27(3):919–933.
- [22] Han B, Chao J, Yao H. Circular RNA and its mechanisms in disease: from the bench to the clinic. *Pharmacol Ther.* 2018;187:31–44.
- [23] Gokool A, Anwar F, Voineagu I. The landscape of circular RNA expression in the human brain. *Biol Psychiatry.* 2020;87(3):294–304.
- [24] Liang ZZ, Guo C, Zou MM, et al. circRNA-miRNA-mRNA regulatory network in human lung cancer: an update. *Cancer Cell Int.* 2020;20(1):173.
- [25] Han TS, Hur K, Cho HS, et al. Epigenetic associations between lncRNA/circRNA and miRNA in hepatocellular carcinoma. *Cancers (Basel).* 2020;12(9):2622.
- [26] Saikishore R, Velmurugan P, Ranjithkumar D, et al. The circular RNA-miRNA axis: a special RNA signature

- regulatory transcriptome as a potential biomarker for OSCC. *Mol Ther Nucleic Acids*. 2020;22:352–361.
- [27] Ye J, Li J, Zhao P. Roles of ncRNAs as ceRNAs in gastric cancer. *Genes (Basel)*. 2021;12(7):1036.
- [28] Kong Y, Li Y, Luo Y, et al. circNFIB1 inhibits lymphangiogenesis and lymphatic metastasis via the miR-486-5p/PIK3R1/VEGF-C axis in pancreatic cancer. *Mol Cancer*. 2020;19(1):82.
- [29] Li Z, Yanfang W, Li J, et al. Tumor-released exosomal circular RNA PDE8A promotes invasive growth via the miR-338/MACC1/MET pathway in pancreatic cancer. *Cancer Lett*. 2018;432:237–250.
- [30] Xiao Y. Construction of a circRNA-miRNA-mRNA network to explore the pathogenesis and treatment of pancreatic ductal adenocarcinoma. *J Cell Biochem*. 2020;121(1):394–406.
- [31] Sun W, Liu R, Li P, et al. Chicken gga-miR-1306-5p targets Tollip and plays an important role in host response against *Salmonella enteritidis* infection. *J Anim Sci Biotechnol*. 2019;10(1):59.
- [32] Chen X, Li C, Li J, et al. Upregulation of miR-1306-5p decreases cerebral ischemia/reperfusion injury in vitro by targeting BIK. *Biosci Biotechnol Biochem*. 2019;83(12):2230–2237.
- [33] Zheng J, Tan Q, Chen H, et al. lncRNASNHG7003 inhibits the proliferation, migration and invasion of vascular smooth muscle cells by targeting the miR13065p/SIRT7 signaling pathway. *Int J Mol Med*. 2021;47(2):741–750.
- [34] Yoshioka H, Wang YY, Suzuki A, et al. Overexpression of miR-1306-5p, miR-3195, and miR-3914 inhibits ameloblast differentiation through suppression of genes associated with human amelogenesis imperfecta. *Int J Mol Sci*. 2021;(4):2202.
- [35] Wang Z, Zhong C, Cao Y, et al. LncRNA DANCR improves the dysfunction of intestinal barrier and alleviates epithelial injury by targeting miR-1306-5p/PLK1 axis in sepsis. *Cell Biol Int*. 2021;45(9):1935–1944.
- [36] Zheng X, Huang M, Xing L, et al. The circRNA circSEPT9 mediated by E2F1 and EIF4A3 facilitates the carcinogenesis and development of triple-negative breast cancer. *Mol Cancer*. 2020;19(1):73.
- [37] Jiang Y, Zhou J, Zhao J, et al. The U2AF2 /circRNA ARF1/miR-342-3p/ISL2 feedback loop regulates angiogenesis in glioma stem cells. *J Exp Clin Cancer Res*. 2020;39(1):182.
- [38] Li H, Shen S, Ruan X, et al. Biosynthetic CircRNA_001160 induced by PTBP1 regulates the permeability of BTB via the CircRNA_001160/miR-195-5p/ETV1 axis. *Cell Death Dis*. 2019;10(12):960.